

# Simple and complex models for studying muscle function in walking

**Marcus G. Pandy**

*Department of Biomedical Engineering, ENS 610, University of Texas at Austin, Austin, TX 78712, USA  
(pandy@mail.utexas.edu)*

While simple models can be helpful in identifying basic features of muscle function, more complex models are needed to discern the functional roles of specific muscles in movement. In this paper, two very different models of walking, one simple and one complex, are used to study how muscle forces, gravitational forces and centrifugal forces (i.e. forces arising from motion of the joints) combine to produce the pattern of force exerted on the ground. Both the simple model and the complex one predict that muscles contribute significantly to the ground force pattern generated in walking; indeed, both models show that muscle action is responsible for the appearance of the two peaks in the vertical force. The simple model, an inverted double pendulum, suggests further that the first and second peaks are due to net extensor muscle moments exerted about the knee and ankle, respectively. Analyses based on a much more complex, muscle-actuated simulation of walking are in general agreement with these results; however, the more detailed model also reveals that both the hip extensor and hip abductor muscles contribute significantly to vertical motion of the centre of mass, and therefore to the appearance of the first peak in the vertical ground force, in early single-leg stance. This discrepancy in the model predictions is most probably explained by the difference in model complexity. First, movements of the upper body in the sagittal plane are not represented properly in the double-pendulum model, which may explain the anomalous result obtained for the contribution of a hip-extensor torque to the vertical ground force. Second, the double-pendulum model incorporates only three of the six major elements of walking, whereas the complex model is fully 3D and incorporates all six gait determinants. In particular, pelvic list occurs primarily in the frontal plane, so there is the potential for this mechanism to contribute significantly to the vertical ground force, especially during early single-leg stance when the hip abductors are activated with considerable force.

**Keywords:** gait determinants; ground force; modelling; muscle; moment; joint

## 1. INTRODUCTION

There is great range in the complexity of mathematical models used to study human walking. Cavagna *et al.* (1976) introduced the simplest of all models, the inverted pendulum, to understand the changes in kinetic and potential energy that occur when humans walk at their natural speeds. The same model has been used more recently to explain the observed changes in duty factor and ground force pattern with walking speed (Alexander 1991, 1992, 1995); to study the dependence on leg stiffness of vertical movements of the centre of mass in walking and running (Lee & Farley 1998); to simulate the time of swing in walking at normal speed (Mochon & McMahon 1980); and to study stability of walking in the absence of active muscle control (McGeer 1990; Garcia *et al.* 1998). At the other end of this spectrum, models of exceeding complexity have been built to learn more about how muscles coordinate motion of the body segments in normal locomotion (Morrison 1970; Yamaguchi & Zajac 1990; Anderson & Pandy 2001; Neptune *et al.* 2001; Pandy 2001; Zajac 2002).

One of the great virtues of a simple model is that it

possesses only a few variables. The fewer the variables, the easier it is to understand the relationships between cause and effect. There are limitations to this approach, however. While the inverted pendulum predicts (correctly) that fluctuations in kinetic and potential energy oppose one another in normal walking, it also produces a ground force pattern that does not correlate with experiment. Force plate records of people walking at their natural speeds show two peaks of vertical force with an intervening minimum. The inverted pendulum predicts just one force peak at midstance, when the leg is perpendicular to the ground.

Many scientists have also built models with multiple joints that are actuated by net moments rather than by muscles (Onyshko & Winter 1980; Mena *et al.* 1981; Pandy & Berne 1988, 1989; Taga 1995). Although these models have added much to our understanding of the mechanics of normal walking, they do not provide detailed information about the functional roles of individual muscles during the gait cycle.

Nonetheless, simple models can be helpful in identifying some basic features of muscle function, as this paper will illustrate. Two very different models of walking, one simple and one complex, are used to study how muscle forces, gravitational forces and centrifugal forces (i.e. forces arising from motion of the body joints) combine

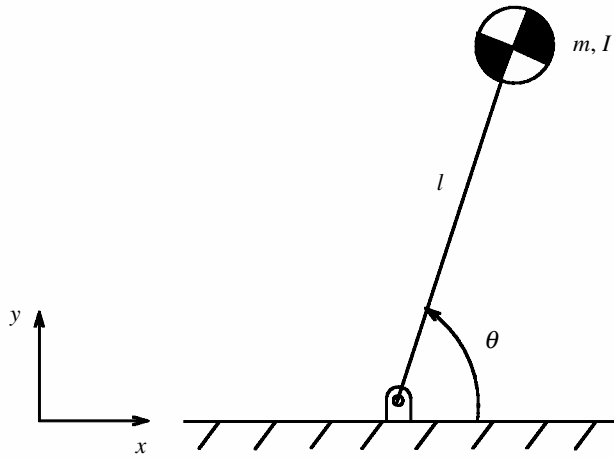


Figure 1. Inverted single pendulum used to model the single-leg stance phase of normal walking. Symbols are defined in Appendix A.

to produce the ground force pattern observed in normal walking. A very simple model of walking, the inverted double pendulum, is used first to show how muscles contribute significantly to the appearance of the two peaks in the vertical ground force. A much more complex, muscle-actuated model of the body is then used to describe how individual muscles contribute to the pattern of force exerted on the ground in normal gait. While the double pendulum model is helpful in uncovering two basic features of leg-muscle function in walking, its predictions are also apt to mislead. Differences in the results obtained from these two models are probably explained by the difference in model complexity.

## 2. INVERTED SINGLE PENDULUM

We will show first that the inverted pendulum is not an appropriate model for studying vertical movements of the centre of mass, and therefore ground force patterns, in walking. In the model in figure 1, the centre of mass is constrained to move on a circular arc, the radius of which is equal to leg length,  $l$ . The vertical position of the mass centre can be written in terms of leg angle,  $\theta$ , quite simply as

$$y_{cm} = l \sin \theta. \tag{2.1}$$

Differentiating equation (2.1) twice with respect to time, multiplying by mass, and adding body weight gives the vertical ground force (see equation (A 2) in Appendix A). If the angular acceleration of the leg is eliminated using the equation of motion for the pendulum, an expression can be written for the vertical force in which the only remaining variables are leg angle and leg angular velocity (equation (A 5) in Appendix A),

$$F_{gy} = -ml \sin \theta \dot{\theta}^2 + mg \sin^2 \theta. \tag{2.2}$$

The values of leg angle and leg angular velocity were calculated by assuming initial values for these variables (i.e. values at the instant of CTO which marks the beginning of single-leg stance), and then integrating the equation of motion for the single pendulum (equation (A 1) in Appendix A) over the entire period of single-leg stance. The values of leg angle and leg angular velocity at each instant

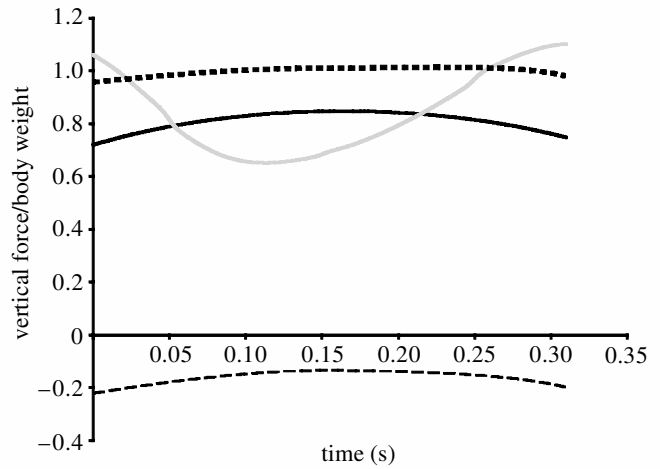


Figure 2. Contribution of the gravitational force (heavy dashed line) and of the centrifugal force (light dashed line) to the vertical ground force (total, heavy solid line) generated by the inverted single pendulum model of figure 1. The grey line is the result recorded by a force plate when humans walk at their natural speeds on level ground. The experimental force-plate data are from Winter (1990).  $t = 0$  s marks the beginning of single-leg stance (contralateral toe-off), and  $t = 0.31$  s marks the end of single-leg stance (contralateral heel strike). All forces are normalized by body weight, which is 567 N for the model and experiment.

during the single-leg stance phase were then input into equation (2.2) to calculate the corresponding vertical ground force. Anthropometric parameters for the model were taken from Winter (1990) (see table 1 in Appendix A).

Because the leg remains close to upright in normal walking,  $\theta \approx 90^\circ$  and  $\sin \theta \approx 1$ . Equation (2.2) then reduces to

$$F_{gy} \approx -ml \dot{\theta}^2 + mg. \tag{2.3}$$

For forward progression, the angular velocity of the leg is positive ( $\dot{\theta} > 0$ ), and so the vertical force always remains below body weight. Indeed, as walking speed increases, the pendulum model predicts smaller and smaller vertical forces, opposite to what is found from experiment (Alexander & Jayes 1978). Thus, the magnitude of the vertical force predicted by the inverted pendulum is inherently different from that observed in human locomotion (see figure 2).

The shape of the vertical force predicted by the inverted pendulum is also opposite to what force records show. Force-plate records of humans walking at their self-selected speeds show two peaks of vertical force: one appearing immediately after CTO; the other just prior to CHS (figure 2, expt). By comparison, the vertical force calculated from the pendulum model shows two minima at the beginning and end of single-leg stance, with an intervening maximum at midstance (compare total and expt in figure 2). The reason for this difference can be seen by looking more closely at equation (2.2). Assuming that no moment acts at the ankle, at midstance, when the leg is vertical,  $\theta = 90^\circ$ ,  $\sin \theta = 1$ , the angular velocity of the pendulum,  $\dot{\theta}$ , is minimum, and  $F_{gy}$  is maximum. For any other angle of the leg (i.e. when  $\theta \neq 90^\circ$ ),  $\sin \theta < 1$  and the magnitude of  $F_{gy}$  decreases from its maximum value at midstance (figure 2, total).

The single pendulum also shows that gravity contributes much more to the vertical ground force than do motion-dependent (centrifugal) forces (figure 2, compare gravity and centrifugal with total). Centrifugal forces do not contribute much to the vertical ground force because the angular velocity of the leg is relatively small in normal walking (i.e. the forward velocity of the centre of mass is only *ca.*  $1.3 \text{ m s}^{-1}$ ). Indeed, centrifugal forces actually act to reduce the vertical ground force because these forces are directed away from the centre of rotation of the leg (i.e. the ankle joint in figure 1), and ultimately away from the ground. Gravitational forces, by comparison, depend only on the position of the leg, and because the leg remains nearly upright in walking, gravity's contribution is almost body weight in the single pendulum model (see equation (2.3)).

### 3. INVERTED DOUBLE PENDULUM

Mochon & McMahon (1980) and Pandy & Berme (1988) extended the inverted pendulum model by attaching a compound pendulum to the hip to simulate knee flexion in swing. The ground force predicted by this triple pendulum is similar to that calculated for the single pendulum in figure 2 (solid heavy line; total), indicating that the pattern of vertical force is not explained by the behaviour of the swing leg alone. This, in turn, suggests that the vertical ground force pattern is determined mainly by the dynamics of the stance leg.

While the compound pendulum has been used repeatedly to simulate the behaviour of the swing leg (Beckett & Chang 1968; Mena *et al.* 1981; Davy & Audu 1987; Piazza & Delp 1996), rarely has it been employed to explain how stance-leg mechanisms contribute to the ground force pattern in normal walking (Siegler *et al.* 1982; Pandy & Berme 1988, 1989).

At the beginning of single-leg stance, just after the contralateral leg has left the ground, the stance-leg knee begins to move into extension and continues to do so, mainly under the action of the quadriceps (Perry 1992). In late single-leg stance, just prior to CHS, the stance-leg ankle plantarflexes rapidly owing to heavy activity in the soleus and gastrocnemius (Winter 1987; Perry 1992). These two observations suggest that stance-knee flexion and stance-ankle plantarflexion are the main mechanisms contributing to the two peaks in the vertical ground force.

Figure 3 shows an inverted double pendulum that may be used to model the single-leg stance phase of walking. Because the contralateral leg is not represented explicitly in this model, double-leg stance is excluded from consideration here. Joint moments and segmental kinematics (i.e. segmental angular displacements and segmental angular velocities) measured for normal walking by Winter (1990) (see Appendix A in Winter (1990)), together with segmental anthropometry also reported by Winter (1990) (see table 2 in Appendix A), were input into equations (A 12), (A 13) and (A 14) of Appendix A to calculate the angular accelerations of the shank, thigh and upper body, respectively. The calculated values of angular accelerations were then used respectively in equations (A 17) and (A 15) to obtain the vertical accelerations of the masses

and the corresponding ground force (see § Ab in Appendix A for details).

The time-course of the vertical ground force is plotted in figure 4 (solid heavy line; model), together with the experimental trace obtained from a force plate. Consistent with the experimental result, the double pendulum predicts two peaks of force separated by a minimum at midstance. The second peak is not as high and the minimum is not as deep as the experimental result, but what is clear is that this behaviour is fundamentally different from that given by the single pendulum (compare solid heavy lines in figures 2 and 4). Perhaps most significantly, the vertical force obtained from the double pendulum rises above body weight in early and in late single-leg stance, whereas the result predicted by the single pendulum remains below body weight for the duration of single-leg stance.

Muscle moments contribute most significantly to the vertical ground force in both early and late single-leg stance (figure 4, moment). Gravitational forces contribute no more than 0.6 body weight near midstance, compared with a maximum of almost one body weight for the single pendulum (compare gravity in figures 2 and 4). Centrifugal forces contribute little throughout the single-leg stance phase, in much the same way as is predicted by the single pendulum model (figure 4, centrifugal).

Gravity's contribution to the vertical ground force is really the passive resistance offered by the rigid segments (shank and thigh) to the downward force of gravity. The fact that gravity contributes less than body weight in figure 4 does not mean that gravity exerts a force that is less than body weight; indeed, gravity always exerts a force that is equal to one body weight. Gravity's contribution in figure 4 represents the vertical ground force that would arise if the body were acted on by gravity alone. For the double pendulum model, the magnitude of gravity's contribution to the vertical ground force depends on the orientations of the shank and thigh segments relative to the ground (i.e.  $\theta_1$  and  $\theta_2$  in figure 3). In any activity, the downward force of gravity is resisted by compressive forces that are transmitted by the bones and joints to the ground. In walking, gravity's contribution to the vertical ground force is maximum at midstance because the leg is nearly vertical at this time. When the leg is vertical, the knee is fully extended, and, in this position, the leg is able to resist the downward force of gravity more effectively. In early and late single-leg stance, however, gravity's contribution decreases to less than one-half of body weight because the leg is then slightly more bent, leading to a greater downward acceleration of the centre of mass and, therefore, a smaller vertical force transmitted to the ground.

The pattern of vertical ground force predicted by the double pendulum is explained by the variation in the net muscle moments applied at the joints. The results of the analysis suggest that the first peak is caused mainly by an extensor moment acting at the knee, whereas the second peak is due almost entirely to a plantarflexor moment applied at the ankle (figure 5, ankle and knee). The model calculations suggest further that an extensor moment applied at the hip will contribute *negatively* to (i.e. reduce) the vertical force exerted on the ground throughout single-leg stance (figure 5, hip).

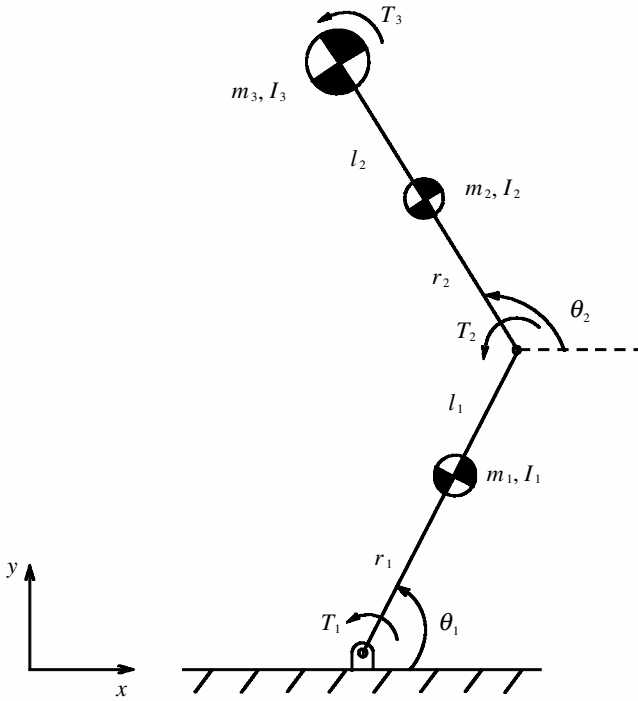


Figure 3. Double inverted pendulum used to model the single-leg stance phase of normal walking. The upper-body segment, mass  $m_3$ , comprises the mass of the head, arms, trunk and swing leg. Note that the upper-body mass can rotate independently of the thigh segment.  $T_1$  and  $T_2$  are the net muscle moments applied at the ankle and knee, respectively.  $T_3$  is the moment at the hip applied to rotate the upper body; its reaction moment simultaneously accelerates the thigh segment. All other symbols are defined in Appendix A.

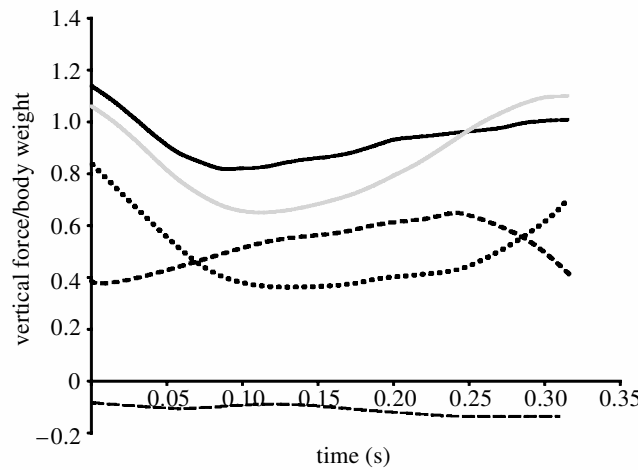


Figure 4. Contributions of gravitational forces (heavy dashed line), of centrifugal forces (light dashed line) and of the net muscle moments acting at the joints (moment, heavy dotted line) to the vertical ground force (total, heavy solid line) generated by the inverted double pendulum model of figure 3. Also shown is the vertical ground force recorded when humans walk at their natural speeds (grey line (Winter 1990)). All forces are normalized by body weight, which is 567 N for the model and experiment.

**4. MUSCLE-ACTUATED MODEL OF WALKING**

If the predictions of the inverted double pendulum are correct, they should be supported by results obtained from

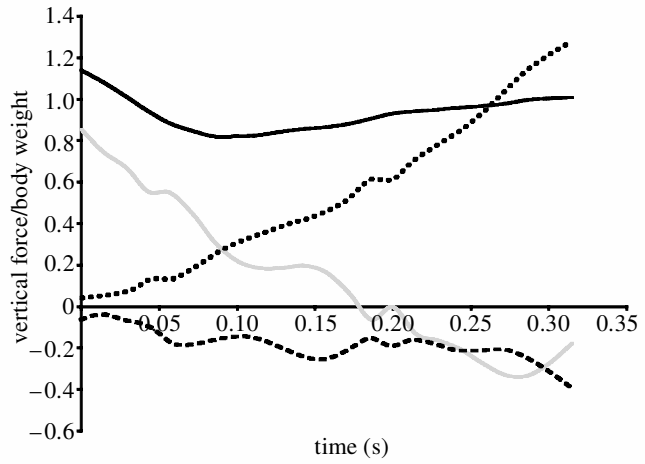


Figure 5. Contributions of the net muscle moments exerted about the ankle (dotted line), knee (grey line) and hip (dashed line) to the vertical ground force generated by the inverted double pendulum model of figure 3 (total, heavy solid line). All forces are normalized by body weight, which is 567 N for the model and experiment.

a more elaborate model of the body. In particular, one would expect a more detailed, muscle-actuated model to also show that muscle forces contribute significantly to the pattern of vertical ground force, and further, that the appearance of the first and second peaks correlate with the actions of the knee extensors and ankle plantarflexors, respectively.

A very complex, 3D musculoskeletal model of the body was built to evaluate the contributions of individual muscles to the ground force pattern in normal walking. The model included all six determinants of normal walking: hip flexion, stance-knee flexion, stance-ankle plantarflexion, transverse pelvic rotation, pelvic list and lateral pelvic displacement (Saunders *et al.* 1953). The skeleton was represented as a 10-segment, 23-degree-of-freedom mechanical linkage (figure 6). The first six degrees of freedom defined the position and orientation of the pelvis relative to the ground. The remaining nine segments branched out in an open chain from the pelvis. The head, arms and torso were represented as a single rigid body that articulated with the pelvis via a ball-and-socket joint located at the level of the third lumbar vertebra. Each hip was modelled as a ball-and-socket joint having three degrees of freedom: hip flexion; internal-external rotation (which permits transverse pelvic rotation); and abduction-adduction (which permits pelvic list). Each knee was modelled as a single degree-of-freedom hinge joint, allowing only flexion and extension. Each ankle-subtalar complex was modelled as a universal joint with two degrees of freedom: ankle plantarflexion and subtalar inversion-eversion (which contributes to lateral pelvic displacement). Each foot was represented by two segments: a hindfoot and a toes segment, hinged together by a single-degree-of-freedom metatarsal joint. Five damped springs were placed under each foot to model the interaction of the feet with the ground (Anderson & Pandy 1999, 2001).

The model skeleton was actuated by 54 muscles: 24 muscles per leg plus 6 abdomen and back muscles. Each muscle was represented by a contractile element with realistic force-length-velocity properties, and series- and

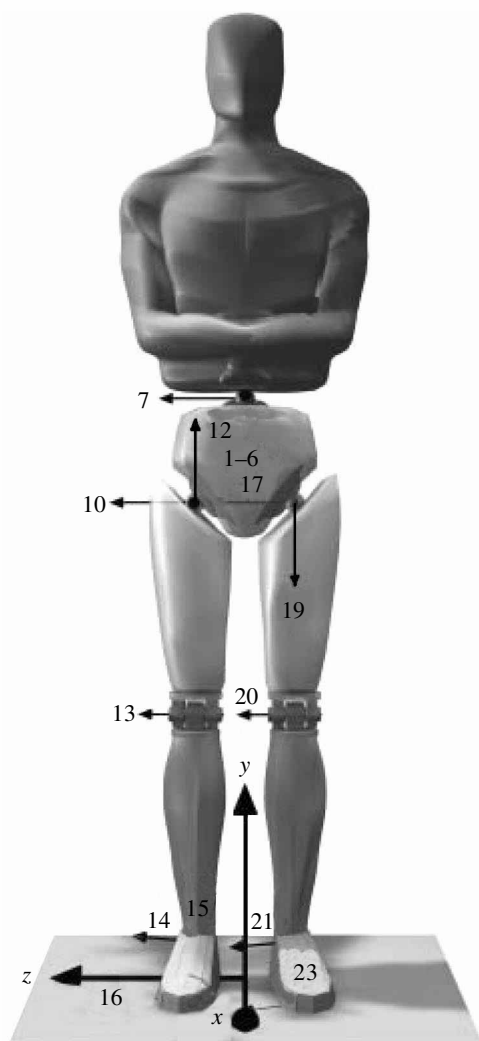


Figure 6. Schematic of the three-dimensional model used to simulate one full cycle (single- and double-leg stance phases) of normal walking (Anderson & Pandy 2001). The inertial reference frame was fixed to the ground at the level of the floor. The  $x$ -axis was directed forward, the  $y$ -axis upwards and the  $z$ -axis laterally. There were a total of 23 generalized coordinates in the model, each labelled as a number in the diagram. Generalized coordinates  $q_1$ – $q_3$  specified the translation of the pelvis with respect to the origin of the inertial frame; and  $q_4$ – $q_6$  were body-fixed Euler angles that specified the orientation of the pelvis with respect to the ground. The relative orientations of the head–arms–trunk segment, right thigh and left thigh with respect to the pelvis were specified using body-fixed Euler angles at the back ( $q_7$ – $q_9$ ), right hip ( $q_{10}$ – $q_{12}$ ) and left hip ( $q_{17}$ – $q_{19}$ ), respectively. The model was actuated by 54 muscles: 24 muscles per leg plus six abdominal and back muscles (not shown). The uniarticular muscles crossing the back joint were erector spinae, external abdominal obliques and internal abdominal obliques on the medial and lateral sides of the body. Uniarticular muscles crossing each hip were iliopsoas, adductor longus brevis, adductor magnus, anterior gluteus medius and anterior gluteus minimus, posterior gluteus medius and posterior gluteus minimus, medial gluteus maximus and lateral gluteus maximus. Biarticular muscles crossing the hip and the knee on each side of the body were tensor fasciae latae; sartorius; gracilis; semimembranosus, semitendinosus and biceps femoris long head lumped together; rectus femoris; piriformis; and pectinius. Uniarticular muscles crossing each knee were vastus medialis, vastus intermedius and vastus lateralis lumped together, and biceps femoris short head. Gastrocnemius was the only biarticular muscle that crossed the knee and ankle on each side of the body. Uniarticular muscles crossing each ankle were soleus, peroneus longus and peroneus tertius and extensor digitorum, tibialis anterior and extensor hallucis longus, tibialis posterior, flexor digitorum longus, flexor hallucis longus, flexor digitorum longus/brevis, flexor hallucis longus/brevis, extensor digitorum longus/brevis and extensor hallucis longus/brevis. See Anderson & Pandy (1999, 2001) for details of the musculoskeletal model.

parallel-elastic elements with active and passive stiffness properties. Tendon was assumed to be elastic. Ligament action was also included by exerting torques at the joints to prevent anatomically infeasible joint angles from arising during the simulation. Muscle excitation–contraction dynamics was represented as a first-order process (Zajac 1989).

Normal walking was simulated by solving a dynamic optimization problem, which minimized the metabolic energy consumed by all the muscles in the model per unit distance travelled (Anderson & Pandy 2001). Metabolic energy was calculated by summing the heat liberated during muscle contraction and the mechanical work done by the muscles to move the joints (Bhargava *et al.* 2003). Because the walking cycle was assumed to be symmetric, it was necessary to simulate only half a cycle. The initial conditions for the simulation were found by averaging kinematic data obtained from five subjects who walked in the laboratory at their natural speeds. The walking cycle was also assumed to be repeatable, in which case the terminal conditions for the simulation were the same as the initial states. The dynamic optimization problem was solved using parameter optimization and high-performance parallel computing. All computations were performed on either an IBM SP-2 or a Cray T3E (Pandy *et al.* 1992; Anderson *et al.* 1995).

The joint angles, ground forces and muscle activation patterns predicted by the dynamic optimization solution were similar to measurements obtained from gait experiments performed on the five subjects (Anderson & Pandy 2001).

Consistent with the predictions of the inverted double pendulum, the walking simulation results show that the leg muscles make the largest contribution to the vertical ground force. Gravitational forces contribute no more than one-half of body weight, and the centrifugal forces remain relatively small throughout single-leg stance (figure 7) (Anderson & Pandy 2003).

From foot-flat to just after CTO, the model GMAX, VAS and GMEDP contribute most significantly to the vertical ground force (figure 8a). These muscles are responsible for the first peak seen in early single-leg stance. Gravity and the hip abductors, GMEDP and GMEDA, contribute nearly all of the vertical force exerted on the ground in midstance (figure 8b), while the ankle plantarflexors, SOL and GAS, are responsible for the second peak just prior to CHS (figure 8c).

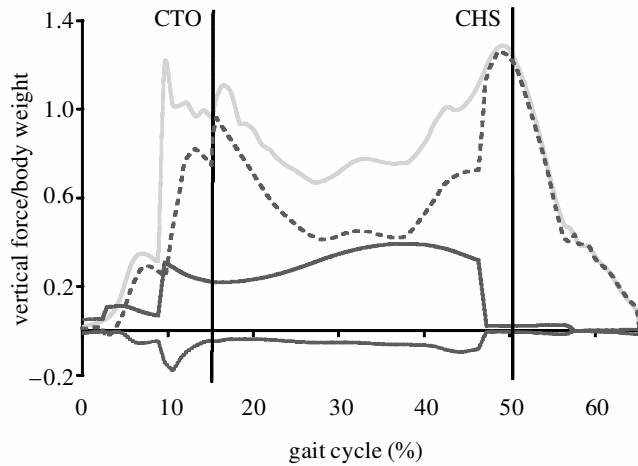


Figure 7. Contributions of gravitational forces (heavy solid line), of centrifugal forces (light solid line), and of muscle and ligament forces (light dashed line) to the vertical ground force (total, grey line) predicted by the 3D, muscle-actuated model of figure 6. The sudden changes in the calculated forces are due to the interaction of the model foot with the ground. Specifically, sudden changes in force occur when the model foot is flat on the ground, when the heel leaves the ground, and when the metatarsals leave the ground. All forces are normalized by body weight, which is 696 N for the walking model. (Adapted from Anderson & Pandy (2003).)

## 5. DISCUSSION AND CONCLUSIONS

Although simple models can be helpful in explaining some basic features of movement, they are also apt to mislead. The inverted double pendulum provides some clues about function of the leg muscles in normal walking, and these results are generally supported by those obtained from a much more complex, muscle-actuated model of the body. Both models show how muscles contribute most significantly to the appearance of the two peaks in the vertical ground force. The double pendulum suggests further that the first and second peaks are due to net extensor muscle moments exerted about the knee and ankle, respectively. Simulation results obtained from a 23-degree-of-freedom, 54-muscle model of walking support the idea that the second peak is due to the action of the ankle plantarflexors, SOL and GAS, but they also show that the knee and hip extensors, VAS and GMAX, contribute equally to the first peak (compare hip in figure 5 with GMAX and VAS in figure 8*a*). Indeed, the more complex model suggests that the hip abductors also contribute significantly to the vertical ground force in early single-leg stance (compare hip in figure 5 with GMEDP in figure 8*a*).

The discrepancy in these findings is not surprising considering the significant difference in structure and complexity of the two models studied. The double pendulum model is planar, has two degrees of freedom, and is actuated by torques rather than by muscles. The walking model, however, is fully 3D, possesses 23 degrees of freedom, and is actuated by 54 muscles, with each muscle having realistic physiological properties. Furthermore, the double pendulum incorporates only three of the six major elements of walking: hip flexion, stance-knee flexion and stance-ankle plantarflexion. Net joint moments are

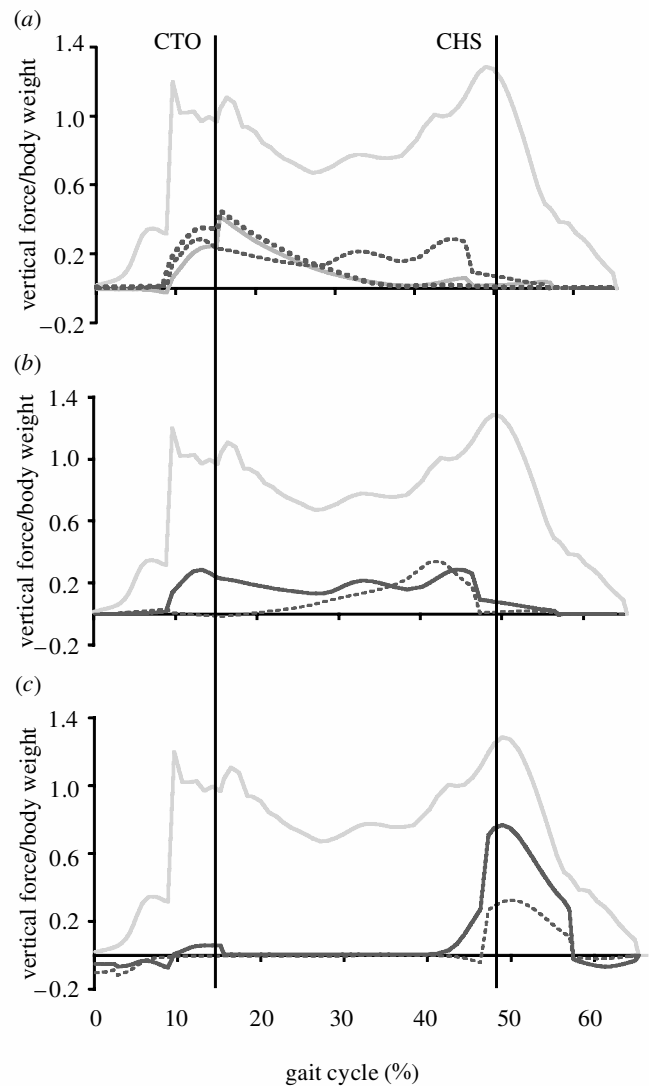


Figure 8. Muscles contributing most significantly to the vertical ground force predicted by the walking model of figure 6. The light grey line in each figure is the vertical ground force obtained from the dynamic optimization solution of normal walking (Anderson & Pandy 2001). Shown are the major contributions made by the leg muscles during one full cycle of normal walking. The sudden changes in the calculated forces are due to the interaction of the model foot with the ground. Single-leg stance occurs between CTO and CHS. Ligaments represents the combined contribution of all ligaments in the model. Ligament action at a joint was represented in the model by exerting a torque at the joint when the joint approached full extension (e.g. at the knee just prior to contralateral heel strike). This was done to prevent the joint from hyperextending during the simulation. The combined contribution of all the ligaments in the model to the vertical ground force was generally much smaller than the combined contribution of the muscles. All forces are normalized by body weight, which is 696 N for the walking model. (a) GMAX, dotted line; VAS, solid line; GMEDP, dashed line. (b) GMEDP, heavy solid line; GMEDA, dashed line. (c) SOL, heavy solid line; GAS, dashed line. Adapted from Anderson & Pandy (2003).

exerted about the hip, knee and ankle to simulate the effect of these three mechanisms on the vertical ground force. However, the fact that an extensor moment applied

at the hip contributes negatively to the vertical ground force (figure 5, hip) suggests that the first determinant, hip flexion, is not properly accounted for in the double-pendulum model. Indeed, even movements of the upper body in the sagittal plane are not represented properly in this model, which may explain the contradictory result obtained for hip-muscle function.

By contrast, the more detailed 3D walking model incorporates all six gait determinants as defined by Saunders *et al.* (1953), and it also represents the actions of all the major uni- and biarticular muscles crossing the ankle, knee, hip and back. This model accounts for movements of the pelvis and trunk in the frontal and transverse planes, controlled in a large part by muscles that cross the hip and back. It is unlikely that transverse pelvic rotation and lateral pelvic displacement contribute significantly to the vertical acceleration of the centre of mass, and therefore to the vertical ground force, because these movements occur mainly in the transverse plane. Pelvic list, however, occurs in the frontal plane, so there is the potential for this mechanism to contribute substantially to the vertical ground force, particularly in early single-leg stance when the hip abductors are activated with considerable force.

## APPENDIX A

### (a) *Single pendulum*

The simplest model capable of walking, the inverted pendulum, has the following equation of motion (see figure 1)

$$(ml^2 + I) \ddot{\theta} + mgl \cos \theta = 0, \quad (\text{A } 1)$$

where  $m$ ,  $l$  and  $I$  are the mass, length and moment of inertia of the pendulum, respectively;  $g$  is the gravitational acceleration at the Earth's surface ( $9.81 \text{ m s}^{-2}$ ); and  $\theta$  is the angle that the pendulum makes with the ground. The vertical component of the ground-reaction force is given simply by

$$F_{\text{gy}} = m\ddot{y}_{\text{cm}} + mg, \quad (\text{A } 2)$$

where  $\ddot{y}_{\text{cm}}$  is the acceleration of the centre of mass of the body, which sits at the tip of the pendulum. The acceleration of the centre of mass can be expressed in terms of the angle,  $\theta$ , angular velocity,  $\dot{\theta}$ , and angular acceleration,  $\ddot{\theta}$ , of the leg:

$$\ddot{y}_{\text{cm}} = l(\cos \theta \ddot{\theta} - \sin \theta \dot{\theta}^2). \quad (\text{A } 3)$$

Using equation (A 3) in (A 2) we can write

$$F_{\text{gy}} = mg + ml(\cos \theta \ddot{\theta} - \sin \theta \dot{\theta}^2). \quad (\text{A } 4)$$

Solving for the angular acceleration of the leg from equation (A 1) and substituting the result into equation (A 4) leads to the following expression for the vertical force:

$$F_{\text{gy}} = -ml \sin \theta \dot{\theta}^2 + mg \sin^2 \theta. \quad (\text{A } 5)$$

The contributions of gravity,  $mg \sin^2 \theta$ , and of the centrifugal force,  $-ml \sin \theta \dot{\theta}^2$ , to the vertical ground force are plotted in figure 2. Table 1 gives the values of the parameters assumed for the inverted single-pendulum model.

Table 1. Parameters assumed for the inverted single-pendulum model of figure 1.

( $\theta|_{t=0}$  is the value of the leg angle,  $\theta$ , assumed at the beginning of single-leg stance (i.e. at time  $t=0$  s). Similarly,  $\dot{\theta}|_{t=0}$  is the value of the leg angular velocity,  $\dot{\theta}$ , assumed at the beginning of single-leg stance (i.e. at time  $t=0$  s). All other symbols are defined in the text.)

$m = 56.7 \text{ kg}$	$\theta _{t=0} = 105 \text{ deg}$
$l = 0.669 \text{ m}$	$\dot{\theta} _{t=0} = -103 \text{ deg s}^{-1}$
$I = 0 \text{ kg m}^{-2}$	

Table 2. Parameters assumed for the inverted double-pendulum model of figure 3.

(All symbols are defined in the text.)

$m_1 = 2.84 \text{ kg}$	$l_1 = 0.342 \text{ m}$
$m_2 = 7.12 \text{ kg}$	$l_2 = 0.327 \text{ m}$
$m_3 = 46.74 \text{ kg}$	$r_1 = 0.194 \text{ m}$
$I_1 = 0 \text{ kg m}^{-2}$	$r_2 = 0.188 \text{ m}$
$I_2 = 0 \text{ kg m}^{-2}$	
$I_3 = 0.5 \text{ kg m}^{-2}$	

### (b) *Double pendulum*

The double pendulum model shown in figure 3 has two degrees of freedom. Mass  $m_3$ , which represents the combined mass of the head, arms, trunk and swing leg, is free to rotate relative to the thigh segment, which is represented by mass  $m_2$ . Mass  $m_3$  is given a moment of inertia to model the resistance to rotation of the upper body about the hip. Free-body diagrams and Newton's second law of motion were used to obtain the following dynamical equations of motion for the double-pendulum model:

$$\begin{aligned} T_1 - T_2 = & (I_1 + m_1 r_1^2 + m_2 l_1^2 + m_3 l_1^2) \ddot{\theta}_1 \\ & + (m_2 l_1 r_2 + m_3 l_1 l_2) \cos(\theta_1 - \theta_2) \ddot{\theta}_2 \\ & + (m_2 l_1 r_2 + m_3 l_1 l_2) \sin(\theta_1 - \theta_2) \dot{\theta}_2^2 \\ & + (m_2 r_1 + m_2 l_1 + m_3 l_1) g \cos \theta_1, \end{aligned} \quad (\text{A } 6)$$

$$\begin{aligned} T_2 - T_3 = & (m_2 l_1 r_2 + m_3 l_1 l_2) \cos(\theta_1 - \theta_2) \ddot{\theta}_2 \\ & + (I_2 + m_2 r_2^2 + m_3 l_2^2) \ddot{\theta}_2 - (m_2 r_2 l_1 + m_3 l_1 l_2) \\ & \sin(\theta_1 - \theta_2) \dot{\theta}_1^2 + (m_2 r_2 + m_3 l_2) g \cos \theta_2 \end{aligned} \quad (\text{A } 7)$$

and

$$T_3 = I_3 \ddot{\theta}_3, \quad (\text{A } 8)$$

where  $T_1$ ,  $T_2$  and  $T_3$  represent the net moments applied at the ankle, knee and hip, respectively;  $m_1$ ,  $m_2$ ,  $m_3$  are the masses of the shank, thigh and upper body, respectively;  $I_1$ ,  $I_2$ ,  $I_3$  are the moments of inertia of the shank, thigh and upper body, respectively;  $l_1$ ,  $l_2$  are the lengths of the shank and thigh, respectively;  $r_1$ ,  $r_2$  are the distances of the centres of mass of the shank and thigh segments from the ankle and knee joints, respectively; and  $\theta_1$ ,  $\theta_2$  are the angles of the shank and thigh segments measured relative to a horizontal line fixed on the ground. Note that  $\theta_3$  is the orientation of the upper-body mass,  $m_3$ , relative to the ground; the mass of the upper body is lumped at the hip. Note also that the hip torque,  $T_3$ , produces an angular acceleration of the upper-body mass  $m_3$ , and that an equal and opposite reaction torque simultaneously produces an angular acceleration of the thigh segment (see equations

(A 7) and (A 8)). Table 2 gives the values of the parameters assumed for the double-pendulum model.

Equations (A 6) and (A 7) may be expressed more simply as

$$T_1 - T_2 = m_{11} \ddot{\theta}_1 + m_{12} \ddot{\theta}_2 + c_{11} \dot{\theta}_1^2 + c_{12} \dot{\theta}_2^2 + g_1 g, \quad (\text{A } 9)$$

$$T_2 - T_3 = m_{21} \ddot{\theta}_1 + m_{22} \ddot{\theta}_2 + c_{21} \dot{\theta}_1^2 + c_{22} \dot{\theta}_2^2 + g_2 g, \quad (\text{A } 10)$$

where the following substitutions have been made:

$$\begin{aligned} m_{11} &= I_1 + m_1 r_1^2 + m_2 l_1^2 + m_3 l_1^2, \\ m_{12} &= (m_2 l_1 r_2 + m_3 l_1 l_2) \cos(\theta_1 - \theta_2), \\ m_{21} &= (m_2 l_1 r_2 + m_3 l_1 l_2) \cos(\theta_1 - \theta_2), \\ m_{22} &= I_2 + m_2 r_2^2 + m_3 l_2^2, \\ c_{11} &= 0, \\ c_{12} &= (m_2 l_1 r_2 + m_3 l_1 l_2) \sin(\theta_1 - \theta_2), \\ c_{21} &= -(m_2 r_2 l_1 + m_3 l_1 l_2) \sin(\theta_1 - \theta_2), \\ c_{22} &= 0, \quad g_1 = (m_2 r_1 + m_2 l_1 + m_3 l_1) \cos\theta_1, \\ g_2 &= (m_2 r_2 + m_3 l_2) \cos\theta_2. \end{aligned} \quad (\text{A } 11)$$

Equations (A 8), (A 9) and (A 10) can be solved for the angular accelerations of the shank, thigh and upper body in terms of the net muscle moments, gravitational forces and centrifugal forces acting on these segments. Thus,

$$\ddot{\theta}_1 = \{m_{22}(T_1 - T_2) - m_{12}(T_2 - T_3) - m_{22} c_{12} \dot{\theta}_2^2 + m_{12} c_{21} \dot{\theta}_1^2 - m_{22} g_1 g + m_{12} g_2 g\} / \det M, \quad (\text{A } 12)$$

$$\ddot{\theta}_2 = \{-m_{21}(T_1 - T_2) + m_{11}(T_2 - T_3) + m_{21} c_{12} \dot{\theta}_2^2 - m_{11} c_{21} \dot{\theta}_1^2 + m_{21} g_1 g - m_{11} g_2 g\} / \det M \quad (\text{A } 13)$$

and

$$\ddot{\theta}_3 = T_3 / I_3, \quad (\text{A } 14)$$

where  $\det M = m_{11} m_{22} - m_{12} m_{21}$ .

From equation (A 2), the vertical ground force is  $F_{gy} = m \ddot{y}_{cm} + mg$ , or alternatively,

$$F_{gy} = m_1 \ddot{y}_1 + m_2 \ddot{y}_2 + m_3 \ddot{y}_3 + mg, \quad (\text{A } 15)$$

where  $\ddot{y}_1, \ddot{y}_2, \ddot{y}_3$  are the vertical accelerations of the shank, thigh and upper body, respectively. The vertical accelerations of these masses can be found by twice-differentiating expressions for their vertical positions. The position equations are

$$\begin{aligned} y_1 &= r_1 \sin\theta_1, \\ y_2 &= l_1 \sin\theta_1 + r_2 \sin\theta_2, \\ y_3 &= l_1 \sin\theta_1 + l_2 \sin\theta_2. \end{aligned} \quad (\text{A } 16)$$

Differentiating equations (A 16) twice gives, respectively,

$$\begin{aligned} \ddot{y}_1 &= r_1 (\cos\theta_1 \ddot{\theta}_1 - \sin\theta_1 \dot{\theta}_1^2), \\ \ddot{y}_2 &= l_1 (\cos\theta_1 \ddot{\theta}_1 - \sin\theta_1 \dot{\theta}_1^2) + r_2 (\cos\theta_2 \ddot{\theta}_2 - \sin\theta_2 \dot{\theta}_2^2), \\ \ddot{y}_3 &= l_1 (\cos\theta_1 \ddot{\theta}_1 - \sin\theta_1 \dot{\theta}_1^2) + l_1 (\cos\theta_2 \ddot{\theta}_2 - \sin\theta_2 \dot{\theta}_2^2). \end{aligned} \quad (\text{A } 17)$$

Substituting equations (A 12) and (A 13) into (A 17) gives the vertical accelerations of the masses as functions of the net muscle moments, the gravitational forces and the centrifugal forces acting on the pendulum. Substituting these expressions into equation (A 15) then gives the contri-

butions of the net muscle moments, the gravitational forces and the centrifugal forces to the vertical force exerted on the ground.

Specifically, the contributions of the joint moments, gravitational forces and centrifugal forces were calculated in three steps. First, joint moments, kinematics (i.e. segmental angular displacements and segmental angular velocities) and segmental anthropometric data reported by Winter (1990) were input into equations (A 12), (A 13) and (A 14) to calculate the angular accelerations of the shank, thigh and upper body, respectively. These values of segmental angular accelerations were then used in equations (A 17) to calculate the contributions of the joint moments, gravitational forces and centrifugal forces to the vertical acceleration of each segment. Finally, the contributions of the joint moments, gravitational forces and centrifugal forces to the vertical accelerations were used in equation (A 15) to find the corresponding contributions to the vertical ground force. The results obtained from these calculations (i.e. the contributions of the joint moments, gravitational forces and centrifugal forces to the vertical ground force) are plotted in figures 4 and 5.

## REFERENCES

- Alexander, R. McN. 1991 Energy-saving mechanisms in walking and running. *J. Exp. Biol.* **160**, 55–69.
- Alexander, R. McN. 1992 A model of bipedal locomotion on compliant legs. *Phil. Trans. R. Soc. Lond. B* **338**, 189–198.
- Alexander, R. McN. 1995 Simple models of human movement. *Appl. Mech. Rev.* **48**, 461–469.
- Alexander, R. McN. & Jayes, A. S. 1978 Vertical movements in walking and running. *J. Zool. Lond.* **185**, 27–40.
- Anderson, F. C. & Pandy, M. G. 1999 A dynamic optimization solution for vertical jumping in three dimensions. *Computer Meth. Biomech. Biomed. Engng* **2**, 201–231.
- Anderson, F. C. & Pandy, M. G. 2001 Dynamic optimization of human walking. *J. Biomech. Engng* **123**, 381–390.
- Anderson, F. C. & Pandy, M. G. 2003 Individual muscle contributions to support in normal walking. *Gait Posture* **17**, 159–169.
- Anderson, F. C., Ziegler, J. M., Pandy, M. G. & Whalen, R. T. 1995 Application of high-performance computing to numerical simulation of human movement. *J. Biomech. Engng* **117**, 155–157.
- Beckett, R. & Chang, K. 1968 An evaluation of the kinematics of gait by minimum energy. *J. Biomech.* **1**, 147–159.
- Bhargava, L. J., Pandy, M. G. & Anderson, F. C. 2003 A phenomenological model for estimating energy production in muscle contraction. *J. Biomech.* (In the press.)
- Cavagna, G. A., Thys, H. & Zamboni, A. 1976 The sources of external work in level walking and running. *J. Physiol.* **262**, 639–657.
- Davy, D. T. & Audu, M. L. 1987 A dynamic optimization technique for predicting muscle forces in the swing phase of gait. *J. Biomech.* **20**, 187–201.
- Garcia, M., Chatterjee, A., Ruina, A. & Coleman, M. 1998 The simplest walking model: stability, complexity, and scaling. *J. Biomech. Engng* **120**, 281–288.
- Lee, C. R. & Farley, C. T. 1998 Determinants of the center of mass trajectory in human walking and running. *J. Exp. Biol.* **201**, 2935–2944.
- McGeer, T. 1990 Passive dynamic walking. *Int. J. Robotics Res.* **9**, 62–82.
- Mena, D., Mansour, J. M. & Simon, S. R. 1981 Analysis and synthesis of human swing leg motion during gait and its clinical applications. *J. Biomech.* **14**, 823–832.



- Mochon, S. & McMahon, T. A. 1980 Ballistic walking. *J. Biomech.* **13**, 49–57.
- Morrison, J. B. 1970 The mechanics of muscle function in locomotion. *J. Biomech.* **3**, 431–451.
- Neptune, R. R., Kautz, S. A. & Zajac, F. E. 2001 Contributions of the individual ankle plantar flexors to support, forward progression, and swing initiation during walking. *J. Biomech.* **34**, 1387–1398.
- Onyshko, S. & Winter, D. A. 1980 A mathematical model for the dynamics of human locomotion. *J. Biomech.* **13**, 361–368.
- Pandy, M. G. 2001 Computer modeling and simulation of human movement. *A. Rev. Biomed. Engng* **3**, 245–273.
- Pandy, M. G. & Berme, N. 1988 Synthesis of human walking: a planar model for single support. *J. Biomech.* **21**, 1053–1060.
- Pandy, M. G. & Berme, N. 1989 Quantitative assessment of gait determinants during single stance via a three-dimensional model. 1. Normal gait. *J. Biomech.* **22**, 717–724.
- Pandy, M. G., Anderson, F. C. & Hull, D. G. 1992 A parameter optimization approach for the optimal control of large-scale musculoskeletal systems. *J. Biomech. Engng* **114**, 450–460.
- Perry, J. 1992 *Gait analysis: normal and pathological function*. Thorofare, NJ: SLACK, Inc.
- Piazza, S. J. & Delp, S. L. 1996 The influence of muscles on knee flexion during the swing phase of gait. *J. Biomech.* **29**, 723–733.
- Saunders, J. B., Inman, V. T. & Eberhart, H. D. 1953 The major determinants in normal and pathological gait. *J. Bone Joint Surg.* **35A**, 543–558.
- Siegler, S., Seliktar, R. & Hyman, W. 1982 Simulation of human gait with the aid of a simple mechanical model. *J. Biomech.* **15**, 415–425.
- Taga, G. 1995 A model of the neuromusculoskeletal system for human locomotion: emergence of basic gait. *Biol. Cybern.* **73**, 95–111.
- Winter, D. A. 1987 *The biomechanics and motor control of human gait*. Waterloo, Ontario: Waterloo Press.
- Winter, D. A. 1990 *Biomechanics and motor control of human movement*. New York: Wiley.
- Yamaguchi, G. T. & Zajac, F. E. 1990 Restoring unassisted natural gait to paraplegics via functional neuromuscular stimulation: a computer simulation study. *IEEE Trans. Biomed. Engng* **37**, 886–902.
- Zajac, F. E. 1989 Muscle and tendon: properties, models, scaling, and applications to biomechanics and motor control. *CRC Critical Rev. Biomed. Engng* **17**, 359–411.
- Zajac, F. E. 2002 Understanding muscle coordination of the human leg with dynamical simulations. *J. Biomech.* **35**, 1011–1018.

## GLOSSARY

- CHS: contralateral heel-strike  
 CTO: contralateral toe-off  
 GAS: gastrocnemius  
 GMAX: medial and lateral portions of gluteus maximus combined  
 GMEDA: anterior gluteus medius/minimus  
 GMEDP: posterior gluteus medius/minimus  
 SOL: soleus  
 VAS: vasti